Published in final edited form as:
Chem Commun (Camb). 2012 December 7; 48(94): . doi:10.1039/c2cc36264c.

Expanding the molecular recognition repertoire of antifreeze polypeptides: effects on nucleoside crystal growth†

Sen Wang[a,‡], **Xin Wen**[*,b], **Pavle Nikolovski**[c], **Vonny Juwita**[b], and **Josh Fnu Arifin**[b]

[a]Molecular Imaging Program, Stanford University, Stanford, 94305, USA

[b]Department of Chemistry and Biochemistry, California State University, Los Angeles, Los Angeles, 90032, USA

[c]Molecular Observatory, California Institute of Technology, Pasadena, 91125, USA

Abstract

Despite differences in the crystal structures of ice and nucleosides, antifreeze polypeptides (AFPs) have been demonstrated to inhibit nucleation of 5-methyluridine, cytidine, and inosine and modify the crystal growth of the nucleosides efficiently. The molecular recognition repertoire of AFPs has been expanded to non-ice-like crystalline solids.

Crystal growth control is essential in various fields in science and technology (*e.g.*, chemistry, materials science, pharmaceutical development).[1–3] The concept of molecular recognition has been successfully used to elucidate the effects of additives (foreign ions or molecules) on crystal growth.[4] Peptides and proteins are often used *in vivo* and *in vitro* to control the growth of minerals and produce new forms of solids with different physicochemical properties.[5–8] Size and shape control of organic crystals, however, is more difficult due to their anisotropic properties (different atomic arrangements in three dimensions).[1,9,10]

Antifreeze polypeptides (AFPs) are a structurally diverse group of proteins found in many cold-adapted organisms (*e.g.*, fish, insect) to protect them from freeze damage through a noncolligative manner, providing an intriguing example of ice crystal growth control. AFPs bind to specific faces of ice crystals and modify the habit of the ice crystals.[11] Their affinity to ice depends on hydrogen bonding and hydrophobic interactions, unlike most protein-mineral interactions where ionic interactions often play a dominant role.[4] Ice and clathrate hydrates (ice-like crystalline solids)[12] are known to be inhibited and modified by AFPs. Nevertheless, we speculate that the recognition ability of AFPs is beyond ice and ice-like crystalline solids based on the facts: (1) ice surfaces are not well ordered at the molecular level compared to other inorganic or organic crystal surfaces[13] and (2) AFPs coexist with many other solutes *in vivo* (*e.g.*, various low molecular solutes present with AFPs in the

†Electronic Supplementary Information (ESI) available: CCDC 835399, Figs. S1–S6, Table S1, and experimental section. For ESI and crystallographic data in CIF or other electronic format see DOI: 10.1039/b000000x/

Fax: + 1 323 343 6490; Tel: + 1 323 343 2310.
‡Visiting scholar at Department of Chemistry and Biochemistry, California State University Los Angeles, Los Angeles, 90032, USA.

§Crystal data for m^5U: $C_{10}H_{14}N_2O_6 \cdot 0.5(H_2O)$ were collected on a Bruker SMART 1000 diffractometer at 100(2) K using 0.71073 Å MoKα. q range for 9892 reflections used in lattice determination: 2.77 to 30.46°; M_r = 267.24; a = 13.9973(5) Å, b = 17.2440(6) Å, c = 4.8028(2) Å, α = β = γ 90°; V = 1159.25(8) Å^3; Z = 4; Orthorhombic; $P2_12_12$; F(000): 564; Total data 30650, independent data 3535 [R_{int} = 0.0432]; Goodness-of-fit on F^2: 2.877; R_1 [$I>2\sigma(I)$] = 0.0318, wR_2 = 0.0554.

hemolymph of *Dendroides canadensis*)[14] diminishing the chance of the growth of single ice crystals.

In this study, we for the first time demonstrate that AFPs can efficiently inhibit the nucleation and modify the single crystal growth of 5-methyluridine (m^5U), cytidine (C), and inosine (I). m^5U, C, and I are widely used nucleosides in pharmaceutical industry, but little is known about their size and shape control using additives.[15–18] This study also presents a distinct example of effective control of nucleoside crystal growths by additives.

We obtained the crystals of m^5U, C, and I, respectively, by evaporation of their aqueous solutions at room temperature (ESI†). The resulting crystals of the three nucleosides appear as orthorhombic needles (Figs. 1a, S2, and S4).[19] The effect of a beetle AFP from *D. canadensis* (DAFP-1) on m^5U crystal growth was first investigated. DAFP-1 is a β-helical repeat protein with a size of 9 kDa containing 8 disulfide bonds, which are important for its structure and function as antifreeze.[20] DAFP-1 was studied previously in our laboratory for its antifreeze enhancement effect by small molecular enhancers and interactions between DAFP-1 and reduced nicotinamide adenine dinucleotide in solution have been demonstrated recently.[21] To completely inhibit single crystal growth, a reasonable additive/nucleoside molar ratio (the critical ratio) is needed. Different amounts of DAFP-1 were added directly to m^5U solution to determine the critical ratio of DAFP-1/m^5U (ESI†). The direct addition of DAFP-1 at all the tested concentrations delayed the first appearances of m^5U precipitates in the solutions (Table S1), while higher additive/m^5U molar ratios resulted in more significant delay. The critical ratio of DAFP-1/m^5U was estimated to be 3.0×10^{-5}, where the ratio is at 3.0×10^{-5} or higher, no single m^5U crystal was detected, but reed-like amorphous m^5U precipitates (Fig. 1b).

Additives usually affect crystal growths through (1) affecting nucleation (*i.e.*, prevent, delay, or promote nucleation); (2) modifying crystal habit (*i.e.*, adsorbing onto specific crystal growing face(s) and changing its growth rate); or (3) both of (1) and (2).[1,22] To further investigate how AFPs affect m^5U crystal growth, DAFP-1 was added to the saturated m^5U solutions in the presence of m^5U seed crystals at the additive/m^5U molar ratio of 1.2×10^{-5}. The growth of m^5U crystals was able to continue, but with an apparent change in the crystal habit, from needle-shaped to normal orthorhombic (Fig. 1c).

Examining by x-ray crystallography, the crystalline m^5U samples in figs. 1a and 1c have the same orthorhombic crystal structure, while no samples in fig. 1b are suitable for single crystal x-ray diffraction (ESI†). In the absence of DAFP-1, the propagation of the needle-like m^5U crystals is along the *a*-axis. The crystal habit is determined by the relative growth rates of different crystal faces, suggesting that the altered crystal habit in the presence of DAFP-1 was caused by selective interaction of DAFP-1 with the (100) faces of m^5U crystals (Fig. 2). The distance between the repeated oxygen atoms in the ribose moieties on the (100) face of m^5U crystal, 4.80 Å (Fig. 2a), matches well to 4.74 Å, the average distance of the hydroxyl oxygen atoms in conserved repeated threonine residues in adjacent loops of DAFP-1,[20] suggesting hydrogen bonding interactions between the hydroxyl groups of the ribose moieties in m^5U crystal and conserved threonines of DAFP-1. Due to such interactions, m^5U crystal growth rate along the *a*-axis decreased to be less than those along the *b*- or *c*-axis, resulting in normal orthorhombic m^5U crystals (Fig. 2b).

The powder X-ray diffraction (PXRD) patterns (Fig. 3a and 3c, ESI†) of the single crystalline m^5U samples in figs. 1a and 1c show the same characteristic peaks assigned to

†Electronic Supplementary Information (ESI) available: CCDC 835399, Figs. S1–S6, Table S1, and experimental section. For ESI and crystallographic data in CIF or other electronic format see DOI: 10.1039/b000000x/

the same unit cell. In contrast, few peaks of very low intensity were observed in the PXRD pattern (Fig. 3b) of the reed-like amorphous m^5U precipitates in fig. 1b, suggesting that these solids lack well-ordered structures, and the few weak peaks that cannot be assigned to any known crystalline phase of m^5U might result from a local order in these m^5U samples.[23] The PXRD results are in good agreement with the single crystal X-ray diffraction data. The finally obtained solids were also analyzed using high performance liquid chromatography (HPLC) to identify whether DAFP-1 presents in the samples (ESI†). The HPLC analysis (Figs. 4b and 4c) indicated the presence of both m^5U and DAFP-1 in the samples in figs. 1b and 1c, suggesting that DAFP-1 is occluded in the reed-like amorphous m^5U precipitates and the normal orthorhombic m^5U crystals, which supports interactions between DAFP-1 and m^5U.

Under the same conditions, m^5U crystal growth was also investigated in the presence of two controls, bovine serum albumin (BSA) and denatured DAFP-1 with complete reduction of its disulfide bonds, respectively (ESI†). Neither BSA nor the denatured DAFP-1 inhibited or delayed the appearance of m^5U precipitates at the control/m^5U molar ratio of 1.8×10^{-4}, a much higher ratio than those used for DAFP-1 (Figs. S1a–b, Table S1). The crystals were characterized to be m^5U by X-ray crystallography and the results were confirmed by PXRD (ESI†). HPLC analysis of these crystals revealed that only pure m^5U presents, suggesting that the controls are simply excluded from the m^5U crystals as impurities (ESI†). These results indicate that the controls have no effect on the crystal growth of m^5U.

To test the generality of the findings, the effect of DAFP-1 and the controls on the crystal growth of two other nucleosides, C and I, were examined. The space groups of m^5U, C and I are all orthorhombic and repeated oxygen atoms in the hydroxyl groups in their ribose moieties are identified on their growing crystal faces, but the dimensions of the unit cells of these nucleosides are quite different.[24–26] The two controls, BSA and the denatured DAFP-1, had no effects on the crystal growth of C and I. Interestingly, the effects of growth inhibition and habit modification were also observed for DAFP-1 on the crystal growth of C and I (Figs. S2–S5, Table S1), suggesting that DAFP-1 can also interact with C and I crystals and such recognition can be flexible. The critical ratios of DAFP-1/C and /I were estimated to be 3.0×10^{-5} and 0.5×10^{-5} (ESI†). To determine whether a different type of AFP can have such effects, all the above experiments were carried out with a globular fish AFP, type III AFP.[27] Similarly, direct additions of type III AFPs in the m^5U, C, and I solutions effectively inhibited the crystal nucleation of m^5U, C, and I, respectively (Figs. S1c, S2f, S4f, Table S1). Additions of type III AFPs in the presence of the seed crystals of m^5U, C, and I, altered the crystal habits of these nucleosides, respectively, and the resulting habits (Figs. S1d, S2g, S4g) are similar to those caused by DAFP-1. However, we did not observe such inhibitory or crystal habit change effect of the AFPs on the crystal growth of thymine, the component base of m^5U, under similar conditions (Fig. S6, ESI†), suggesting that the hydroxyl containing ribose plays an important role in the recognition of m^5U by AFPs.

In conclusion, the inhibitory and habit-modifying effects of AFPs on the stable nuclei formations and on the crystals of nucleosides have been first demonstrated. Such effects of AFPs are analogous to their effects on ice[28] despite the large structural differences among ice I_h and these nucleoside crystals,[24,26,29] suggesting flexibility in AFP molecular recognition. The crystal-recognition repertoire of AFPs has been expanded beyond ice and ice-like crystals. Moreover, the effects of AFPs on the nucleoside crystal growth are highly efficient, comparing with other additives on crystal growth control.[1,22] The results encourage further studies on the roles of AFPs in controlling the crystal growths of polycrystalline ice and other important hydroxyl compounds (*e.g.*, nucleoside analogues, glycosides, sugars) and the use of AFPs, particularly DAFP-1 (which can withstand a wide

range of pHs and temperatures)[30] as scaffolds to design novel, effective crystal growth inhibitors and modifiers in a number of fields including chemistry, materials science, and pharmaceutical industry.

Supplementary Material

Refer to Web version on PubMed Central for supplementary material.

Acknowledgments

The authors thank Prof. John Duman at University of Notre Dame for cDNA of DAFP-1; Dr. Michael Day and Mr. Larry Henling for X-ray crystallographic structural determination and Prof. Mark Davis and Mr. Mark Deimund for PXRD instrument at California Institute of Technology. XW acknowledges support by NIH (GM086249) and Research Corporation (CC10492).

Notes and references

1. Mullin, JW. Crystallization. 4th ed.. Oxford: Butterworth-Heinemann; 2001.
2. Cox JR, Ferris LA, Thalladi VR. Angew. Chem. Int. Ed. 2007; 46:4333–4336.
3. Cölfen H. Angew. Chem. Int. Ed. 2008; 47:2351–2353.
4. Mann, S. Biomineralization: Principles and Concepts in Bioinorganic Materials Chemistry. 1st edition ed.. USA: Oxford University Press; 2002.
5. Belcher M, Wu XH, Christensen RJ, Hansma PK, Stucky GD, Morse DE. Nature. 1996; 381:56–58.
6. Falini G, Albeck S, Weiner S, Addadi L. Science. 1996; 271:67–69.
7. DeOliveira DB, Laursen RA. J. Am. Chem. Soc. 1997; 119:10627–10631.
8. Volkmer D, Fricke M, Huber T, Sewald N. Chem. Commun. 2004:1872–1873.
9. Miller JM, Collman BM, Greene LR, Grant DJ, Blackburn AC. Pharm. Dev. Technol. 2005; 10:291–297. [PubMed: 15926678]
10. Chemburkar SR, Bauer J, Deming K, Spiwek H, Patel K, Morris J, Henry R, Spanton S, Dziki W, Porter W, Quick J, Bauer P, Donaubauer J, Narayanan BA, Soldani M, Riley D, McFarland K. Org. Process Res. Dev. 2000; 4:413–417.
11. Raymond JA, Wilson P, DeVries AL. Proc. Natl. Acad. Sci. U. S. A. 1989; 86:881–885. [PubMed: 2915983]
12. Zeng H, Wilson LD, Walker VK, Ripmeester JA. J. Am. Chem. Soc. 2006; 128:2844–2850. [PubMed: 16506762]
13. Watkins M, Pan D, Wang EG, Michaelides A, VandeVondele J, Slater B. Nat Mater. 2011; 10:794–798. [PubMed: 21892176]
14. Duman JG, Serianni AS. J. Insect Physiol. 2002; 48:103–111. [PubMed: 12770137]
15. Mansuri MM, Starrett JE, Wos JA, Tortolani DR, Brodfuehrer PR, Howell HG, Martin JC. J. Org. Chem. 1989; 54:4780–4785.
16. Gerland, Desire J, Lepoivre M, Décout JL. Org. Lett. 2007; 9:3021–3023. [PubMed: 17608486]
17. Chen P, Goldberg DE, Kolb B, Lanser M, Benowitz LI. Proc. Natl. Acad. Sci. U.S.A. 2002; 99:9031–9036. [PubMed: 12084941]
18. Liu F, You SW, Yao LP, Liu HL, Jiao XY, Shi M, Zhao QB, Ju G. Spinal Cord. 2006; 44:421–426. [PubMed: 16317421]
19. Chiarella RA, Gillon AL, Burton RC, Davey RJ, Sadiq G, Auffret A, Cioffi M, Hunter CA. Faraday Discuss. 2007; 136:179–193. [PubMed: 17955810]
20. Wang S, Amornwittawat N, Juwita V, Kao Y, Duman JG, Pascal TA, Goddard WA, Wen X. Biochemistry. 2009; 48:9696–9703. [PubMed: 19746966]
21. Wen X, Wang S, Amornwittawata N, Houghton EA, Sacco MA. J. Mol. Recognit. 2011; 24:1024–1031.
22. Sangwal, K. Additives and Crystallization Processes: From Fundamentals to Applications. West Sussex, England: John Wiley & Sons Ltd.; 2007.

23. Tremayne M, Kariuki BM, Harris KDM. Angew. Chem. Int. Ed. 1997; 36:770–772.
24. Furberg S, Peterson CS, Romming C. Acta Cryst. 1965; 18:313–320.
25. Hunt DJ, Subramanian E. Acta Cryst. 1969; B25:2144–2152.
26. Munns ARI, Tollin P. Acta Cryst. B. 1970; 26:1101–1113. [PubMed: 5537153]
27. Jia Z, DeLuca CI, Chao H, Davies PL. Nature. 1996; 384:285–288. [PubMed: 8918883]
28. Jia ZC, Davies PL. Trends Biochem. Sci. 2002; 27:101–106. [PubMed: 11852248]
29. Fletcher, NH. The Chemical Physics of Ice. 1 ed.. Cambridge: Cambridge University Press; 1970.
30. Li N, Andorfer C, Duman J. J. Exp. Biol. 1998; 201:2243–2251. [PubMed: 9662495]

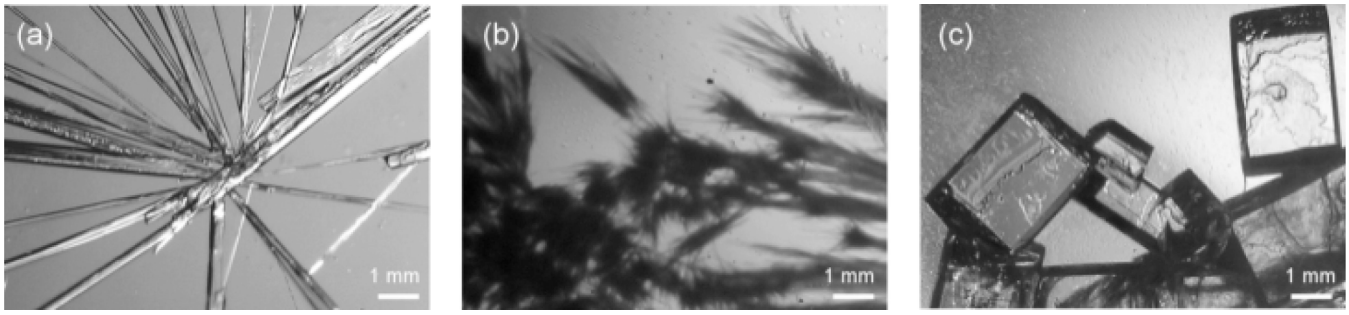

Fig. 1.

Optical micrographs of the finally achieved m^5U solids. (a) Needle-like orthorhombic m^5U crystals, (b) reed-like amorphous m^5U precipitates obtained in the presence of DAFP-1, (c) normal orthorhombic m^5U crystals obtained in the presence of DAFP-1 and m^5U seed crystals.

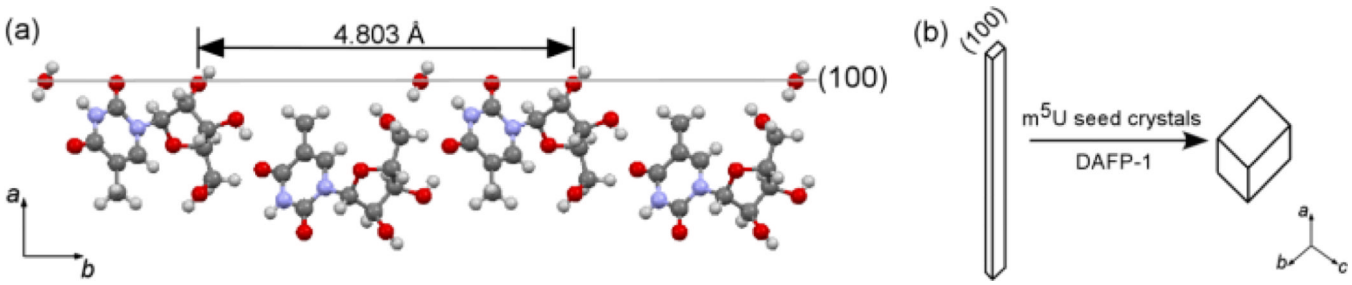

Fig. 2.

(a) The structure of the (100) face of m^5U crystals (carbon, grey; oxygen, red; hydrogen, white; nitrogen, blue). The *c*-axis points into the plane of the paper. (b) Schematic representation: the growth rate along the *a*-axis is much faster than that along the *b*- or *c*-axis in a typical m^5U crystal habit, while the growth along the *a*-axis is significantly inhibited in the presence of DAFP-1 becoming less than that along the *b*- or *c*-axis.

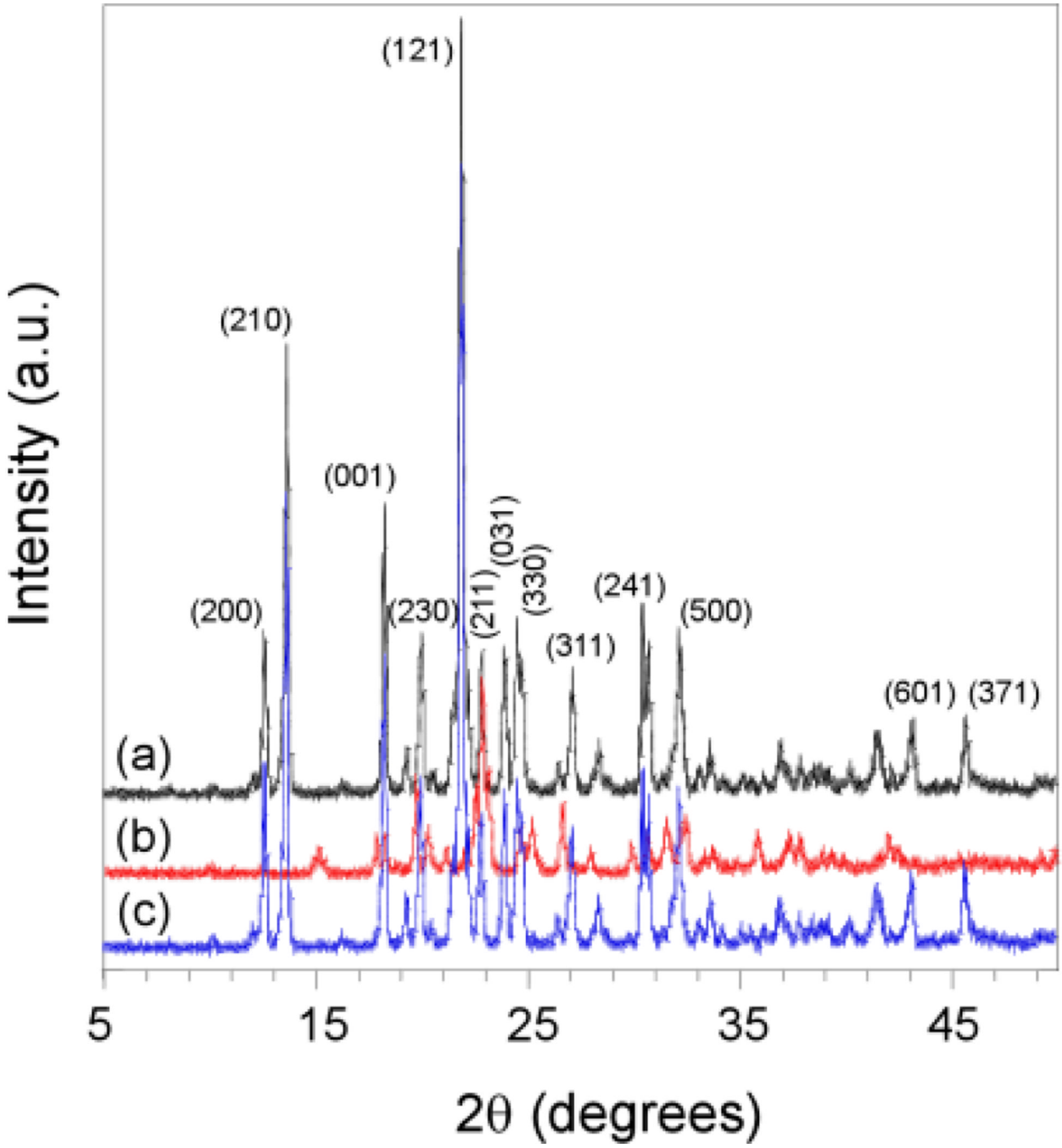

Fig. 3.

Overlay of representative powder XRD profiles of the samples from (a) needle-like crystalline m^5U, (b) reed-like amorphous m^5U precipitates obtained in the presence DAFP-1, and (c) normal orthorhombic crystalline m^5U modified by DAFP-1. Major crystalline peaks in (a) are labeled with miller indexes (*hkl*).

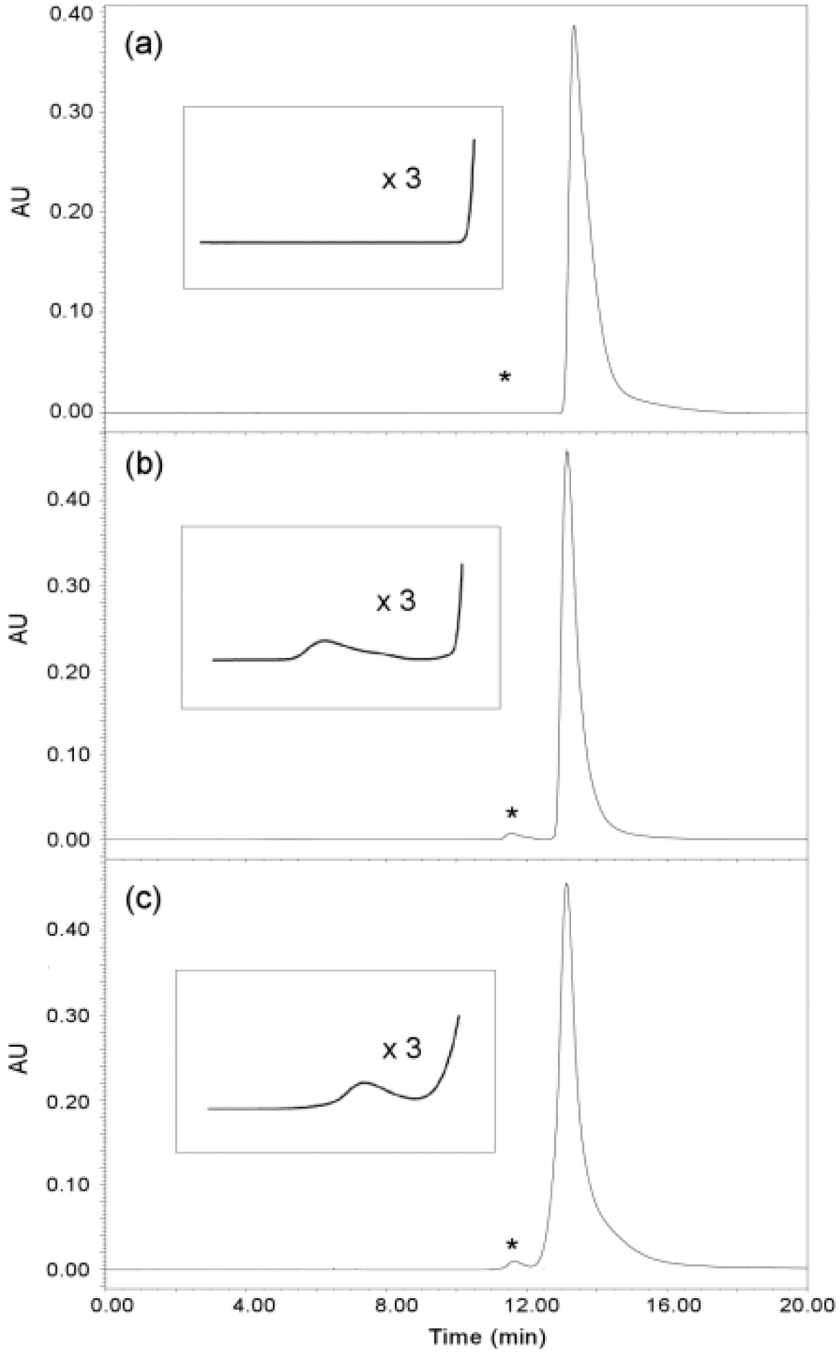

Fig. 4.

Gel filtration HPLC analysis of the crystals of m^5U monitored at 280 nm. Typical chromatograms of (a) crystalline m^5U obtained in the presence of denatured DAFP-1, (b) reed-like amorphous m^5U precipitates obtained in the presence of DAFP-1, (c) normal orthorhombic crystalline m^5U modified using DAFP-1 in the presence of m^5U seed crystals. The retention times for m^5U and DAFP-1 are 13.1 min and 11.5 min, respectively. Insets: enlarged portions (denoted by asterisks).